Journal of Inorganic Biochemistry 200 (2019) 110808

Contents lists available at ScienceDirect

Journal of Inorganic Biochemistry

journal homepage: www.elsevier.com/locate/jinorgbio

Inorganic ions on hemozoin surface provide a glimpse into *Plasmodium* biology

E. Danae Guerra[a], Fadi Baakdah[b], Ophélie Gourgas[a], Mifong Tam[c], Mary M. Stevenson[c,d], Elias Georges[b], D. Scott Bohle[e], Marta Cerruti[a,*]

[a] Department of Mining and Materials Engineering, McGill University, Montreal, Quebec H3A 2B2, Canada
[b] Institute of Parasitology, McGill University, Ste Anne de Bellevue, Quebec H9X 3V9, Canada
[c] Department of Microbiology and Immunology, McGill University, Montreal, Quebec H3A 2B4, Canada
[d] Department of Medicine, McGill University, Montreal, Quebec H4A 3J1, Canada
[e] Department of Chemistry, McGill University, Montreal, Quebec H3A 0C5, Canada

ARTICLE INFO

Keywords:
Hemozoin
Malaria pigment
Surface composition
Inorganic ions
Immune response
Biomineralization

ABSTRACT

In malaria, *Plasmodium* parasites produce hemozoin (Hz) as a route to detoxify free heme released from the catabolism of hemoglobin. Hz isolated from the parasites is encapsulated in an organic layer constituted by parasite and host components. This organic coating may play a role in Hz formation and in the immunomodulatory properties attributed to Hz, and they may influence the mode of action of antimalarials that block Hz formation. In this work, we analyze the organic layer adhered to Hz, and find Na, Cl, Si, Ca and P present, in addition to organic material. Our results suggest that Na, Cl, and P adsorb during Hz release from the red blood cells, while Si and Ca derive from components present during Hz biomineralization within the digestive vacuole of the parasite. Overall, we show that inorganic elements associated with Hz surface provide insights into the biological functions of *Plasmodium* parasites.

1. Introduction

Malaria is a life-threatening disease caused by parasites of the *Plasmodium* genus that are transmitted by the bite of an infected female *Anopheles* mosquito [1]. During the asexual stage of *Plasmodium*, the parasite feeds on hemoglobin, releasing heme inside its digestive vacuole (DV). Free heme can inhibit multiple enzymes, disrupt cell membranes and produce cell lysis [2]. Therefore, to avoid its deleterious effects, the parasite sequesters heme to form an insoluble crystal called hemozoin (Hz), also known as the malaria pigment [1].

Hz crystallization starts with two heme molecules binding through an iron-carboxylate bond forming dimers; the dimers are further linked through hydrogen bonds in a crystalline structure [3]. Although the structure and biochemistry of Hz are mostly understood, its biomineralization process is not completely elucidated at the molecular level, especially the role of different biomolecules in promoting crystal nucleation and growth [4].

Hz is the antimalarial target of the quinoline family of drugs and probably of artemisinins, which exert their effect by interfering with the crystal formation [5]. However, the exact mechanism of action of these drugs is still under debate [6], and the widespread resistance to this class of antimalarials threatens their efficacy [7]. Hz birefringence and optical dichroism [8] are exploited in malaria diagnosis *in vivo* [9]; while its paramagnetic properties serve as a biomarker for malaria diagnosis in blood smears [8]. This property is also extensively used for the separation of infected RBC (red blood cells) from healthy ones *in vitro* [10] and further crystal purification using magnetic separators [11]. In addition, Hz modulates the immune response during malarial infection [6].

The biological activity of Hz and its role in the host immune response is a controversial topic. It is usually tested using Hz synthetic counterpart, hematin anhydride (HA) (also known as β-hematin), or different Hz preparations obtained from *in vitro* or *in vivo* models [12]. However, these reports often produce inconsistent or irreproducible results [13]. For example, one study showed that by cultivating fresh extracts of Hz with monocytes, the cells were unable to mature into

Abbreviations: HA, hematin anhydride; Hz, hemozoin; nHz, native hemozoin; Pf, *Plasmodium falciparum*; Pc, *Plasmodium chabaudi*; CQS, chloroquine-sensitive; CQR, chloroquine-resistant; Mφ, macrophages; RBC, red blood cell; XPS, X-ray photoelectron spectroscopy; SEM, scanning electron microscopy; EDS, energy-dispersive X-ray spectroscopy; NEXAFS, near-edge X-ray absorption fine structure spectroscopy; PDMS, poly(dimethylsilane); Ca pyroP, calcium pyrophosphate

* Corresponding author at: 3610 University Street, 2M020 Wong Building, Montreal, QC H3A 0C5, Canada.
E-mail address: marta.cerruti@mcgill.ca (M. Cerruti).

https://doi.org/10.1016/j.jinorgbio.2019.110808
Received 15 May 2019; Received in revised form 23 August 2019; Accepted 24 August 2019
Available online 27 August 2019
0162-0134/

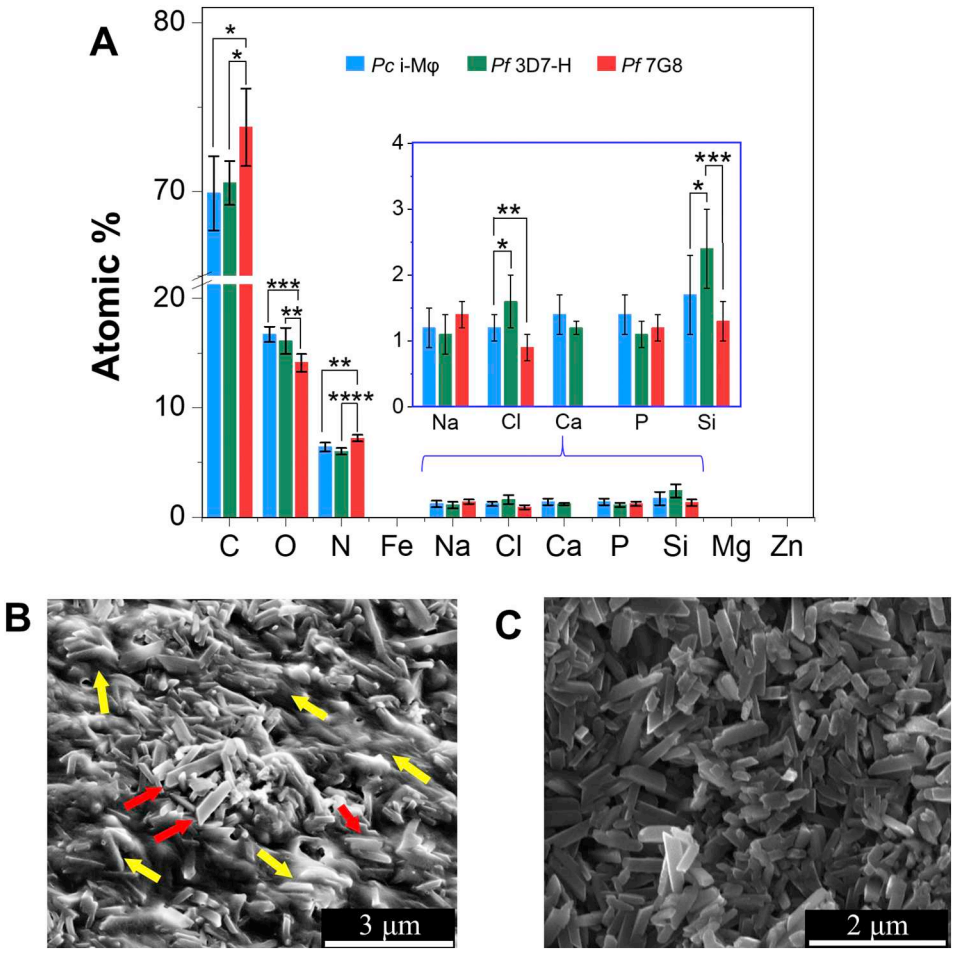

Fig. 1. A) XPS survey collected for nHz samples obtained from CQS *P. chabaudi* AS infected-macrophages (*blue*) and *P. falciparum* of the strains 3D7-H (CQS, *green*) and 7G8 (CQR, *red*). Data represent mean ± SD of 3 independent samples and three different spots analyzed along the same sample. One-way ANOVA test was used for statistical analysis, followed by Bonferroni's test correction to evaluate the statistical difference of multiple samples, where $P < 0.01$ was considered a significant difference All data are expressed as mean ± standard deviation (SD). *Significant differences between atomic percentage, with $^{*}P < 0.01$, $^{**}P < 0.001$, $^{***}P < 1 \times 10^{-5}$and $^{****}P < 1 \times 10^{-6}$. SEM images of B) nHz crystals rinsed with hexane and dichloromethane. The red arrows indicate the crystals devoid of most of the cell components, while the yellow arrows note the crystals still coated with biological residues. C) Clean sample of Hz showing individual crystals lacking most of the organic residues as a result of treatment for proteins precipitation, enzymatic hydrolysis, and rinses with detergents and water, as reported in [18]. Data represent mean ± SD of three independent experiments. (For interpretation of the references to colour in this figure legend, the reader is referred to the web version of this article.)

dendritic cells [14]. Contrary to these observations, another study showed that purified Hz enhanced dendritic cell maturation [15]. Hz also contributes to malarial anemia by suppressing red blood cells (RBC) proliferation *in vivo* [16], but HA shows lower activity compared to Hz [16a]. Also, it was observed that Hz remains unaltered inside macrophages for extended periods, whereas HA is vulnerable to degradation by phagocytosis of macrophages [13].

The differences in biological activity between HA and Hz may be associated with differences in crystal size and morphology [16a]. Additionally, several studies indicate that during the isolation of Hz, the crystals interact with lysed parasitic cells and erythrocytes, whose constituents [17] may ultimately adsorb onto Hz [6], forming a coating that is often considered “contamination” [1]. Some groups have also proposed that this coating is implicated in the immune response associated with Hz [13]; thus, it is not clear whether the immunomodulatory properties of Hz are caused by the crystals or the material adsorbed onto their surface [6]. Furthermore, there are many reported procedures to purify Hz prior to its analysis, which lead to a variety of unidentified biomolecules adsorbed onto Hz that in turn may impact the immunogenic response [6,13,18].

Previous attempts to elucidate the composition of the organic coating adhered onto Hz revealed that it is mainly constituted by proteins, carbohydrates, amino acids, traces of lipids and nucleic acids [17,19]. The amounts of these constituents differ depending on the technique used to purify the crystals since some material is lost or degraded during Hz isolation and treatment [17]. These compounds may be related to components inside the DV of the parasite or the host RBC [6].

Also, the composition of the organic material on Hz surface extracted from *in vitro* cultures may differ from the crystals obtained from *in vivo* models due to several cycles of Hz phagocytosis by circulating monocytes and tissue macrophages [6]. Ingestion of Hz by many generations of phagocytes causes the adsorption of a variety of biomolecules onto its surface, producing Hz with altered morphology and biochemical composition. All of these differences could be responsible for the variable results obtained when evaluating the biological activity of Hz [6].

Finally, while most works debate over the type of biomolecules present in the coatings (lipids, proteins, carbohydrates, *etc.*), our previous study identified Si and Ca in the coating of Hz derived from *in vitro* cultures of *P. falciparum*, [18] and another work mentioned the presence of Ca derived from Ca^{2+}-dependent protein kinase 1 (CDPK1) in DV membranes and the organic material adsorbed on Hz [20]. Nothing is known about the role of these inorganic ions in Hz biomineralization; and their presence could also influence the mode of action of some antimalarials. Also, additional inorganic species could be adsorbed on Hz, which may have been missed by previous reports due to the extensive washing.

Some key questions are thus: what is present on the coating adsorbed on Hz? How does its composition vary among the different models used to grow the parasite? And, more deeply: can we learn something about Hz formation and *Plasmodium* functions by analyzing this layer?

In this work, we answer these questions by studying the composition of the material adhered on Hz obtained from an *in vitro* and an *in vivo* model of *Plasmodium* using a surface-sensitive technique, X-ray photoelectron spectroscopy (XPS), combined with near-edge X-ray absorption fine structure (NEXAFS) and scanning electron microscope (SEM)/energy-dispersive X-ray spectroscopy (EDS). We find that several inorganic ions are consistently present on the surface of all Hz

models we analyzed. To understand the origin of these elements, we compared the elemental species found on Hz and on HA immersed in solutions that simulate the components that may adhere onto Hz during its synthesis and ejection from the RBC. Based on these results, we suggest some hypotheses on the biological function of these elements in *Plasmodium*.

2. Results and discussion

We extracted Hz from chloroquine-sensitive (CQS) *P. chabaudi AS* infected macrophages (Mφ), and *P. falciparum in vitro* cultures of the strains 3D7-H (also CQS) and 7G8 (chloroquine-resistant (CQR)). The materials were washed mildly with organic solvents (Method 3) to remove the parasitic cell debris and host components weakly adhered to the crystals surface, while preserving the components strongly adsorbed. These samples are referred as native hemozoin (nHz) in this work. We used XPS to study the composition of the organic layer adsorbed on the crystals. The overall quantification of the major components on nHz, such as proteins, lipids, and carbohydrates, can be ambiguous since their quantities may differ among models used to collect nHz (*in vitro* and *in vivo*); this may explain the differences in C, N and O observed among samples (Fig. 1A). The variation in washing procedures also account for such differences, as we previously showed using hematin anhydride as a model [18]. For this reason, in this study we focused on identifying the elements present on nHz and their chemical speciation. The XPS analysis of these samples (Fig. 1A) showed the presence of C, O, and N, but no Fe. This implies that the mild washes with hexane and dichloromethane were not sufficient to eliminate all the organic coating and expose a "pure" Hz surface. This was confirmed by SEM (Fig. 1B), which showed Hz crystals coated by a thin shroud of organic matter, in contrast to Hz treated with enzymes and detergents after isolation (Fig. 1C). This result implies that the signals of C, O, and N arise from organic contamination involving not only proteins but also cell debris constituted by traces of C and O-rich lipids and carbohydrates, rather than the porphyrin ring of Hz [17]. This is also confirmed by the finding of the unexpected inorganic elements Na, Cl, P and Si in all the samples, and additionally Ca in Hz collected from *P. chabaudi*-infected murine macrophages and *Pf* 3D7-H strain.

The fact that the inorganic species are present on the surface of all nHz samples regardless of the source suggests that these elements are introduced during Hz biomineralization, or its egress during schizogony or from the RBC. Calcium was not found on the surface of one of the nHz collected from *in vitro* cultures probably due to the strain of *P. falciparum* used to collect the Hz. The absence of Mg and Zn on the surface of all the samples of nHz indicates that nucleic acids are not present in significant amounts [18] as these ions are typically arranged within the structure of DNA and RNA [21].

We previously reported the presence of Si and Ca on the surface of Hz samples washed with solvents, proteinase K in an alkaline buffer, and detergents [18]; however, we did not detect any Na, Ca, or P on these samples. This shows that Si and Ca adsorb strongly on Hz, while P, Na, and Cl are just weakly adsorbed on the outer layer of the crystal, along with organic material. Therefore, Si and Ca may be introduced in the DV of the parasite, while Na, Cl, and P may adsorb during the release of Hz from the DV and RBC. In the same study, we extended the cleaning procedure of Hz using alkaline buffers to dissolve the outermost layers of the crystals; however, we did not detect inorganic elements after this procedure. This showed that the inorganic elements are present on the surface of Hz, and not within the crystalline structure.

To study the spatial distribution of the inorganic elements associated with nHz, we collected EDS maps of samples of nHz produced from *in vitro* cultures of *P. falciparum* strain 3D7-H. These samples were rinsed with water to remove any excess ions present in the extraction buffers (Methods S6.1). Fig. 2A shows the crystals encapsulated in the organic layer. The EDS map of nHz showed the presence of C, O, N, Fe, characteristic of Hz, as well as Na, Cl, Si, Ca, and P, confirming the XPS data. EDS detected Fe (Fig. 2B) because it is a less surface sensitive technique than XPS, sampling approximately 0.2–1 μm [22] rather than the 3–10 nm analyzed by XPS [23].

The EDS maps showed a close correlation between the location of C and Ca (Fig. 2C and D, respectively), but no correlation between Ca and P. This indicates that Ca may be present in an organic environment. Si appears distributed evenly along the whole area mapped in small quantities, while Na and Cl are present in the spots lacking C and Ca. This suggests the presence of adsorbed Na and Cl salts on the organic layer of Hz.

To determine if the inorganic elements found in nHz derive from parasitic debris, we studied the surface composition of *P. falciparum* parasites of the 3D7-H strain, rinsed with the same organic solvents used to prepare nHz (Methods S1). XPS analysis showed Na, Cl, Si and P (Fig. S1), indicating that these elements indeed may originate from the parasites themselves. Na^+ and Cl^- are ions commonly found within the parasite, erythrocytes and the buffers used to extract Hz [24]; therefore, it is not surprising to find these elements associated with nHz and the parasites, probably as undissolved NaCl salts left after the rinses with organic solvents. However, XPS did not detect any significant amount of Ca on *Plasmodium* parasites, possibly because this element is found mostly within parasitic organelles, which are beyond the sampling limit of surface-sensitive XPS [18].

In the following sections, we focus on understanding the speciation of Ca, Si and P found on nHz as a means to understand their possible origins.

2.1. Atomic environment of silicon

The XPS Si_{2p} spectra of nHz obtained from *P. falciparum* 3D7-H cultured *in vitro* showed two peaks located at 102.0 ± 0.1 and 103.0 ± 0.1 eV (Fig. 3A). The peak located at 103.0 eV has been related to Si in SiO_2 [25] or Si in carbon-silica composites [26]; while the peak at 102.0 eV has been assigned to Si in a more reduced state. These same results were obtained for nHz collected from different species of *Plasmodium* in an *in vitro* and an *in vivo* model (Fig. S2). The signal at 102 eV is also close to Si in vacuum grease used to seal the vacuum system in XPS; however, this sort of contamination would be consistently present in all the samples of nHz and in the controls involving HA. Also, the additional signal at around 103 eV in the Si_{2p} spectra of all nHz and *Plasmodium* parasites would not be present in a Si_{2p} peak originating from vacuum grease.

To determine if the observed Si derives from the parasite cultivation media or the process of Hz extraction, we suspended HA in blood serum, RBC membranes and in the buffers used to lyse the parasites (Methods S5.1). The XPS survey spectra did not show any Si on these samples (Fig. S3), suggesting that the Si on nHz is most likely parasite-derived. To confirm this hypothesis, we analyzed *Plasmodium* parasites (Methods S1). The Si_{2p} spectra of this sample (Fig. 3B) showed two signals located at 101.9 ± 0.2 and 103.1 ± 0.2 eV, identical to the peaks found in nHz ($P = 0.17$ and $P = 0.27$, respectively).

To understand the origin of the two observed Si species on nHz and *Plasmodium*, we suspended HA crystals in different solutions containing Si compounds and studied the chemical environment of the Si_{2p} signal coming from the crystal surface afterward. First, we suspended HA in a solution of silicic acid (Methods S5.2), also known as hydrated silica ($Si(OH)_4$); this compound is slightly soluble in water and is naturally adsorbed by vascular plants [27]. The Si_{2p} spectrum on this sample (Fig. 3C) showed a peak centered at higher energy (104.2 ± 0.0 eV, $P = 5.2 \times 10^{-11}$) that the peaks found on nHz (Fig. 3A), suggesting that the Si species found on the organic coating of Hz do not contain silicic acid.

Next, we evaluated cucumber skin (*Cucumis sativus*) since this plant is Si-rich. The XPS Si_{2p} analysis of this sample (Fig. 3D) revealed two peaks located at 101.9 ± 0.1 and 103.2 ± 0.3 eV at positions very close to those found on nHz ($P = 0.25$ and $P = 0.34$). We analyzed also

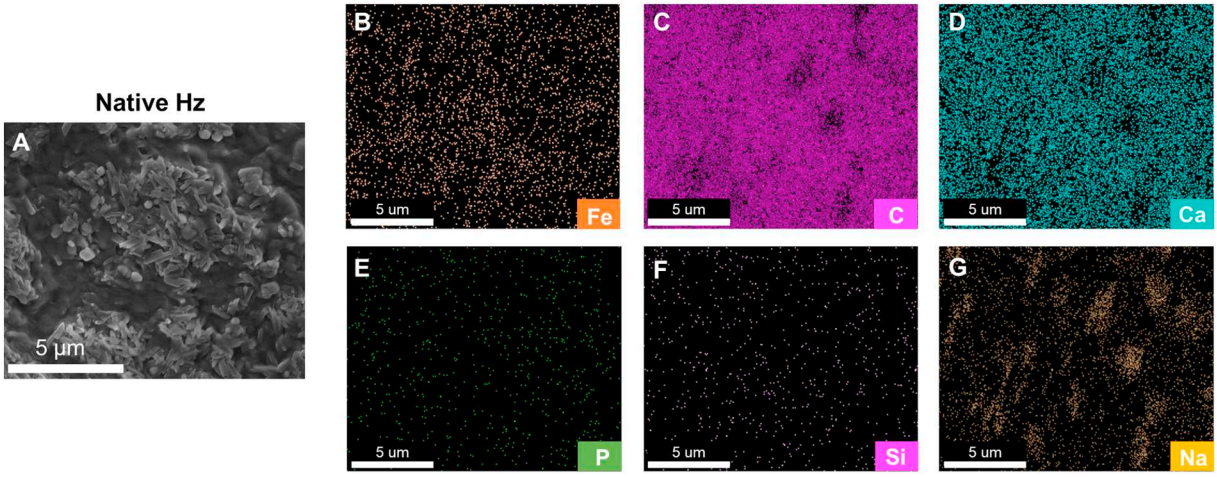

Fig. 2. A) Scanning electron microscopy (SEM) images of nHz obtained from *P. falciparum* strain 3D7-H and energy-dispersive X-ray spectroscopy (EDS) elemental mapping for B) Fe, C) C, D) Ca, E) P, F) Si and G) Na.

the branch of another Si-rich plant commonly known as horsetail (*Equisetum hyemale*) and obtained similar results ($P = 0.06$ and $P = 0.79$, with respect to nHz) (Fig. 3E). The XPS Si_{2p} signals of both plants are very close to those found on nHz surface, which suggests that the Si-species in these two plants are similar or equivalent to those found on nHz. In addition, the location of the 102.0 eV peak has been reported for compounds containing SiO_4^{4-} anions in the form of oligomerized hydrated silica in studies of silicon-substituted apatites [28].

The peak at approximately 102 eV could also correspond to silicon oxycarbide compounds in the form of SiO_3C and SiO_2C_2 [29]. To explore this option, we suspended HA in a solution of poly(dimethylsilane) (PDMS) (Methods S5.3), a polymer containing a silicon oxycarbide (SiO_2C_2) bond in its structure. The XPS Si_{2p} spectrum of this sample revealed a single peak centered at 102.0 ± 0.0 eV (Fig. 3F). This analysis highlights the unusual biochemistry of the Si species associated with nHz. Since no other groups ever reported Si in *Plasmodium* parasites, we can only hypothesize its physiological role. In plants, Si enhances the activity of the enzymes responsible for the defense against biotic stress due to pathogen attacks, and abiotic stresses such as drought, temperature, salinity, and metal toxicity [30]. Hence, Si is required for the growth and development of many plants species [30a].

In diatoms, the metabolism of silicic acid is also vital for structural growth; they incorporate Si into the cell wall to form a structure called frustule [31]. Diatoms possess intracellular pools of soluble silicon at supersaturated concentrations, ranging from 19 to 340 mM, depending on the diatom species and the water content within the cell [31]. This silicon is maintained solubilized by interaction with organic components to produce mono-silicic acid or low molecular weight poly-silicic

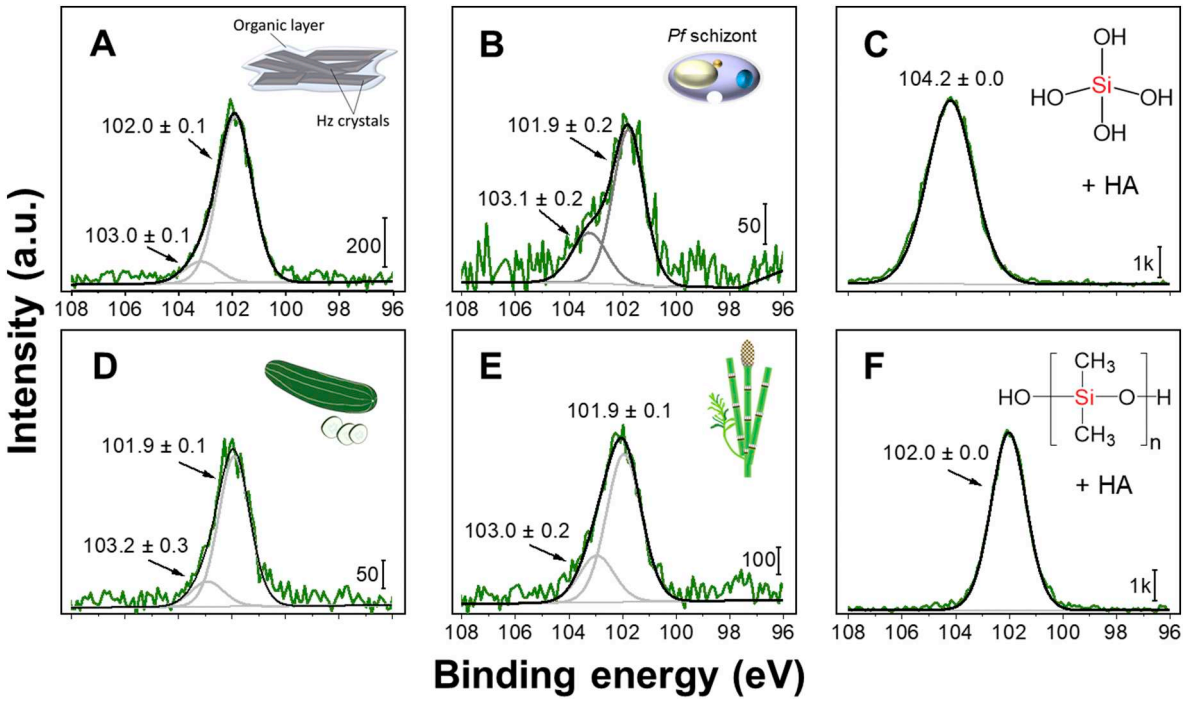

Fig. 3. XPS high-resolution spectra of Si_{2p} collected for A) Hz extracted from *P. falciparum* of the strain 3D7-H, B) *P. falciparum* parasites of the strain 3D7-H, C) HA suspended in silicic acid, D) cucumber skin (*Cucumis sativus*), E) horsetail (*Equisetum hyemale*) and F) HA suspended in PDMS (Mn~550). Experimental data is shown in green, peaks fit in gray, and the overall fit in black. (For interpretation of the references to colour in this figure legend, the reader is referred to the web version of this article.)

acid bound to biological components [31–32].

In mammals and some fruits, Si is found covalently bound to the backbone of some polysaccharides through Si-O-C links formed between silicic acid and hydroxyl groups, resulting in a bridge of Si-O-C, *i.e.* as an ether (or esther) [33]. The Si-O-C link formed between silicic acid and hydroxyl groups is highly resistant to diluted alkali and acid. However, strong alkali and acid hydrolyze the Si-polysaccharide bond, releasing the silicon in the form of SiO_2 [33]. This observation suggests that the two Si_{2p} signals arising from nHz and *Plasmodium* may derive from Si bound to intracellular components of the parasite, as reported for diatoms and mammals. Thus, the Si_{2p} contribution at 102.0 eV could be related to Si in Si-O-C bonds due to Si covalently bonded to carbohydrates, which were previously found on nHz [17], or to oligomerized hydrated silica. Meanwhile, the Si_{2p} signal at 103.2 eV could result from SiO_2 released from the partial hydrolysis of covalently bonded Si due to the acidic conditions of the DV.

It is possible that the parasite acquires silicon compounds from the host blood [34] as it is estimated that humans and other mammals average 0.5 mg of silicon per liter of blood plasma [27a]. Based on these reports and our Si_{2p} spectra analysis, we hypothesize that inside the parasite Si may be present as soluble oligomerized hydrated silica chains, or bound to cell components such as polysaccharides, in addition to some SiO_2.

Since silica particles are known to cause an acute inflammatory response [35], the presence of Si on Hz surface could contribute to the immune modulation attributed to the crystals during malaria infection.

2.2. Atomic environment of calcium

We used both XPS and NEXAFS to study the atomic environment of calcium. The XPS high-resolution spectra of Ca_{2p} of nHz from *P. falciparum* 3D7-H (Fig. 4A) showed the two characteristic peaks associated with the spin-orbit splitting of Ca_{2p}, with the $Ca_{2p3/2}$ peak centered at 347.3 ± 0.1 and the $Ca_{2p1/2}$ peak at 350.7 ± 0.1 eV. As before, we suspended HA in blood serum, RBC membranes and in the buffers used to lyse the parasites (SI Methods S5.1) to determine if Ca came from the parasite culture media or the reagents used for Hz isolation. The XPS survey analyses did not show Ca on the surface of these samples (Fig. S3), indicating that this element is *Plasmodium*-derived. In fact, there are various reserves of Ca^{2+} in the parasite, such as the endoplasmic reticulum, acidocalcisomes, mitochondria, Golgi apparatus, nuclei, and even the DV where Hz is formed [36]. In the intraerythrocytic stage of *Plasmodium*, Ca is found in the DV at an elevated concentration (250–300 nM), which is approximately 5 or 6 times higher than Ca in the cytosol [37]. During schizogony, free Ca^{2+} leaves the DV and redistributes in the intermembranes of each merozoite segment, followed by a rapid decrease in Ca content [37]. Since Hz is also released during schizont rupture, it may come into contact with this element during its egress.

To further understand the origin of the Ca species, we first suspended HA in a solution of calcium acetate (Methods S5.4), as a representative compound for calcium in an organic environment, *e.g.* calcium coordinated to carboxylate groups. The spectrum measured on this sample (Fig. 4B) was very close to that of nHz ($Ca_{2p3/2}$ at 347.3 ± 0.1, $P = 0.86$), confirming that calcium atoms are present within an organic structure. This chemical environment also corresponds to Ca in calcium carbonate, which gives rise to a $Ca_{2p2/3}$ signal at 347.2 eV [38], equivalent to what found in nHz. However, there are not sources of calcium carbonate in the parasite, thus, this compound is unlikely to be associated with nHz.

We also measured the Ca_{2p} spectrum on cucumber skin and found the $Ca_{2p3/2}$ peak at 347.1 ± 0.0 eV, similar to Hz ($P = 0.06$) (Fig. 4C). Plants and some Apicomplexa parasites share common Ca^{2+}-binding proteins [39], and the finding of similar Ca species suggests that the organic coating adhered onto nHz may contain Ca in a similar environment. These results suggest that Ca associated with nHz may be found in an organic matrix or coordinated to cellular components.

Calcium is also present in *Plasmodium* within acidocalcisomes; these acidic organelles serve as storage for cations, amino acids, and concentrated phosphorus [40]. Calcium is pumped in the acidocalcisomes

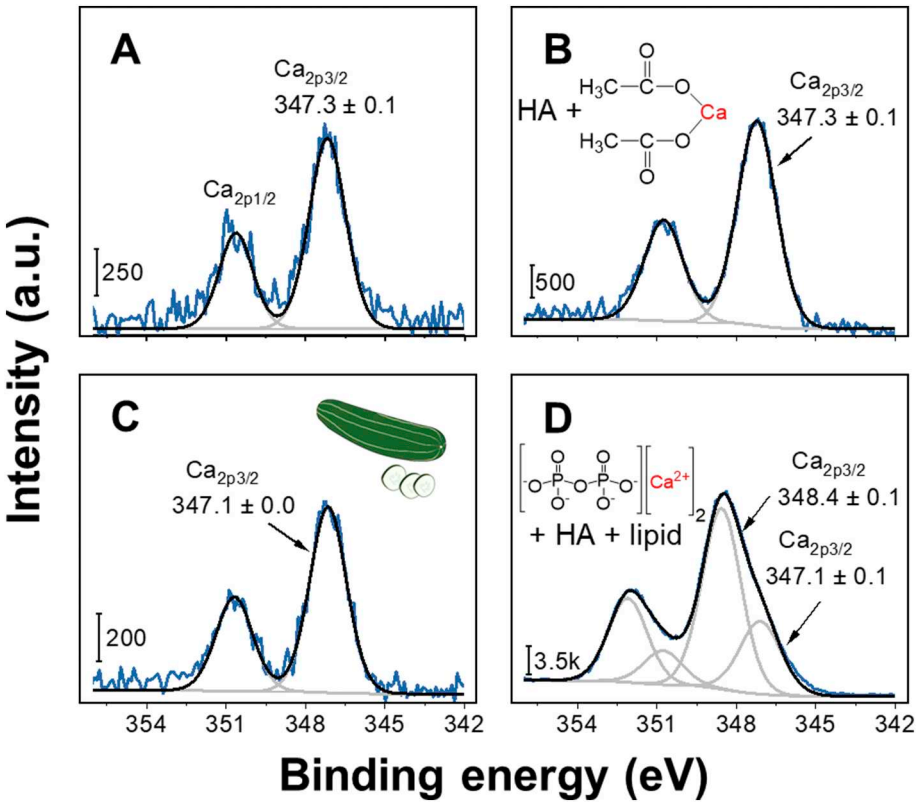

Fig. 4. XPS high-resolution spectra of Ca_{2p} collected for A) Hz extracted from *P. falciparum* of the strain 3D7-H, B) HA suspended in calcium acetate, C) dried cucumber skin (*Cucumis sativus*) and D) HA and calcium pyrophosphate suspended in cholesterol. Experimental data is shown in blue, peaks fit in gray, and the overall fit in black. (For interpretation of the references to colour in this figure legend, the reader is referred to the web version of this article.)

by Ca^{2+}-ATPase, where it is thought to bind to other molecules such as short and long chains of polyphosphate, within an acidic environment [36]. Acidocalcisomes are involved in calcium homeostasis, intracellular pH and osmoregulation in bacteria, mammals, algae and other Apicomplexa besides *Plasmodium*, such as *Schistosoma*, *Toxoplasma, and Trypanosoma* [41].

To determine if the Ca in the nHz coating could be related to Ca complexed with phosphorus from acidocalcisomes, we suspended HA in a solution of calcium pyrophosphate (Ca pyroP) (Methods S5.5). The XPS analysis of this control sample showed no adsorption of Ca pyroP on HA surface (Fig. S5). We hypothesized that this is because the synthetic crystals are devoid of the organic coating that is naturally present on nHz and could act as a binding intermediate.

To test this hypothesis, we evaluated the adsorption of Ca pyroP on HA crystals suspended in cholesterol (Methods S5.6). We selected this lipid to simulate the adherent capacity of the organic material adsorbed on nHz; also, this compound does not contain inorganic elements that could give rise to overlapping signals. In the presence of cholesterol, the calcium pyrophosphate adsorbed onto HA crystals (Fig. 4D). This result shows the importance of an intermediate layer (lipidic in our example, but possibly proteinic too) as a means to adhere insoluble salts or solid particles on Hz.

The XPS analysis of Ca pyroP adhered to HA through cholesterol reveals two different $Ca_{2p3/2}$ signals located at 347.1 ± 0.1 and 348.4 ± 0.1 eV (Fig. 4D). The signal at 347.1 eV is very close to that found on nHz ($P = 0.13$) and is also found in calcium hydrogen phosphate ($CaHPO_4$, Fig. S4A); however, the presence of an additional $Ca_{2p3/2}$ peak indicates that this compound produces Ca in two different chemical states, unlike what we found on nHz. This suggests that Ca pyroP is not likely to be the origin of the Ca found on nHz, confirming the EDS map results that did not show a strong association between Ca and P.

To determine more precisely the composition of the calcium compounds found on nHz, we used Ca K-edge NEXAFS spectroscopy. This technique provides additional information about the geometrical arrangement of neighboring atoms surrounding an atom of interest [42]. To identify the Ca species present in nHz, we selected some reference samples representative of Ca in a variety of environments and performed linear combination fitting (Methods S7.1). Our reference samples included *P. falciparum* parasites of the 3D7-H strain and calcium acetate ($Ca(CH_3COO)_2$) as a model for carboxylated calcium ions.

Fig. S6 shows the spectra obtained for these reference samples. All the samples showed a small pre-edge feature at around 4035 eV arising from the electronic transition from 1s to 3d orbitals [43]. The adsorption edge at around 4040 eV is assigned to the transitions associated with 1s to $4p_{1/2}$ and 1s to $4p_{3/2}$; the relative intensities of the latter peaks are associated with the neighboring atoms surrounding the calcium [44].

The linear combination fitting results (Table S1) showed that the Ca in nHz mostly consists of Ca acetate (around 90%), suggesting that Ca ions are present in an organic matrix, probably as calcium coordinated to carboxylate groups, again confirming both XPS and EDS map results.

Conversely, the analysis of the parasites revealed that only a small proportion of Ca ions are present in the form of calcium coordinated to carboxylate groups. This may be related to the calcium phosphate compounds stored inside the acidocalcisomes in the parasites [41]. More experiments would be needed to confirm this due to the low concentration of Ca present in both samples that result in spectra with low signal-to-noise ratio.

2.3. Atomic environment of phosphorus

The XPS analysis of P_{2p} of nHz collected from *P. falciparum* 3D7-H cultured *in vitro* showed two peaks characteristic of the spin orbit splitting of this element at 133.1 ± 0.1 eV ($P_{2p3/2}$) and at 133.9 ± 0.1 eV ($P_{2p1/2}$), as shown in Fig. 5A. As before, we analyzed the P_{2p} spectra of HA suspended in blood serum, RBC membranes and in the buffers used to lyse the parasites (Methods S5.1). Only phosphorus from RBC membranes adhered on Hz surface, producing a $P_{2p3/2}$ signal at 133.7 ± 0.3 eV (Fig. 5B). The difference between this binding energy and that measured on nHz ($P = 0.005$) suggests that despite the strong affinity of RBC membranes towards HA or Hz crystals [17], the P found on the organic coating of nHz may have a different origin; we hypothesized that it may be *Plasmodium*-derived. In fact, in the asexual stage of *Plasmodium*, P is found in the parasitic membranes in the form of phospholipids, especially phosphatidylcholine [45].

To test this hypothesis, we suspended HA crystals in solubilized phosphatidylcholine (Methods S5.7). The XPS P_{2p} spectrum of this sample (Fig. 5C) showed a $P_{2p3/2}$ peak located at 133.0 ± 0.1 eV, very close to that in nHz ($P = 0.07$), suggesting that phospholipids could adhere to the surface of the crystals when Hz is released from the parasite. These results suggest the presence of phospholipids or phosphorylated proteins derived from parasite structures in the organic layer of nHz, discriminating between possible P-containing contaminants in nHz.

In *Plasmodium,* phosphorus is also associated with the phosphorylation of some proteins. We analyzed the $P_{2p3/2}$ signal from ortho-DL-phosphoserine, as a compound representative of the chemical environment of P in an organic environment. The XPS spectrum (Fig. 5D) shows a $P_{2p3/2}$ signal at 133.2 eV ± 0.1 eV, similar to that measured on nHz ($P = 0.08$), showing that P in nHz could also originate from phosphorylated proteins.

Overall, the similar localization of the $P_{2p3/2}$ peaks of HA suspended in phosphatidylcholine and ortho-DL-phosphoserine suggests that the P associated to nHz might be present as an orthophosphate group (PO_4^{3-}) since this chemical environment is consistent among these samples and their energy is very close to that measured for nHz.

Another source of P in *Plasmodium* is acidocalcisomes [40]. We analyzed two P compounds formed inside acidocalcisomes: sodium polyphosphate, containing phosphoanhydride bonds $(PO_3)_n^{n-}$; and Ca pyroP, bearing $P_2O_7^{4-}$ bonds [41]. Both high-resolution spectra of these compounds are different from that measured on nHz: on Na polyphosphate (Fig. 5E) the $P_{2p3/2}$ signal is at much higher binding energy (134.3 ± 0.1 eV, $P = 1.2 \times 10^{-10}$), while on Ca pyroP we found two $P_{2p3/2}$ peaks at 133.1 ± 0.1 and 134.5 ± 0.1 eV (Fig. 5F). The signal at lower energy is identical to that in nHz ($P = 0.06$) and $CaHPO_4$ (Fig. S7A); however, the presence of an additional $P_{2p3/2}$ peak clearly indicates that this compound is not found in the organic coating of nHz. These results ruled out the presence of deposits from acidocalcisomes on the organic coating of nHz.

3. Conclusions

In this work, we used XPS, NEXAFS, and EDS for the first time to study the elemental composition and speciation of the organic residues adhered to Hz collected from different models of *Plasmodium* and gently washed with organic solvents. We showed that the residues are not only constituted by C, O, and N, but they also contain a variety of inorganic elements, namely Na, Cl, Si, Ca and P. We found these inorganic elements on crystals both extracted from *Plasmodium* obtained from *in vitro* cultures and from macrophages derived from an *in vivo* model of rodents, suggesting that their composition remains unaltered despite the interaction with a variety of cells or culture models. The fact that Ca was not found on the surface of some samples of nHz collected from *in vitro* cultures may be an indication that something is different in the Hz synthesis in the strains of *P. falciparum* used to collect the Hz. More studies should be pursued to explain this observation.

Biomolecules and inorganic elements may adhere to Hz during its biomineralization, its release from the DV or the parasite's egress from RBC. The observation that Ca and Si are strongly adsorbed on Hz suggests that these elements are related to Hz crystallization, whereas the weak adsorption of Na, Cl, and P on Hz surface may occur during the

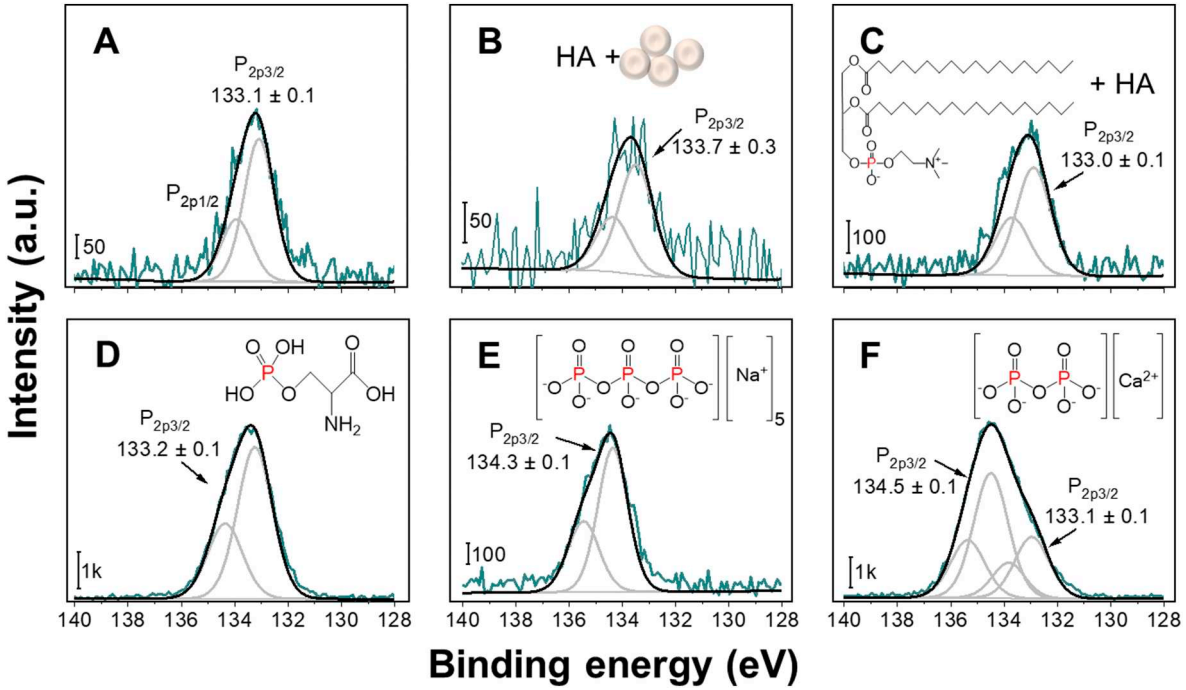

Fig. 5. High-resolution P_{2p} XPS spectra collected for A) Hz extracted from *P. falciparum* of the strain 3D7-H, B) HA suspended in RBC membranes, C) HA mixed with phosphatidylcholine, D) reference sample of *ortho*-DL-phosphoserine, E) sodium polyphosphate, and F) calcium pyrophosphate. Experimental data is shown in teal blue, peaks fit in gray, and the overall fit in black. (For interpretation of the references to colour in this figure legend, the reader is referred to the web version of this article.)

crystal's egress from the DV or RBC.

Even though XPS, EDS, and NEXAFS alone cannot determine the exact biomolecular composition of Hz's coating, our approach involving the use of controls as candidates for the adsorbed species in conjunction with high-resolution XPS spectra analysis has provided us with several crucial insights.

Possibly the most interesting finding from this work was the presence of two different Si species on nHz and on *Plasmodium* parasites of various strains, and its similarity with the Si-species found on Si-rich plants and possibly in mammals. To the best of our knowledge, there are no reports about the absorption of Si by *Plasmodium* or any other parasites; however, this element is essential for the development of plants and some algae with similar evolutionary lines of *Plasmodium* [46], and is required for the normal growth and development of connective tissue and bones in mammals [47]. Several questions arise from these observations: first, what is the pathway, localization and function of Si in the parasite? Second, why is this element present on the surface of Hz? Finally, is it possible that the Si is associated with Hz biomineralization or implicated in the immune modulation of Hz in the host? Unlike Na, Cl, and P, we found Si on Hz surface even after washes with high pH buffers and proteases [18], this suggests that indeed Si may adsorb on Hz within the DV of *Plasmodium*. Our findings suggest that the parasites have reserves of solubilized hydrated silica, or Si bound to cell components, and some SiO_2. Further work is necessary to clarify this intriguing hypothesis and understand how/if it is related to Hz crystallization.

Both XPS and NEXAFS showed that Ca associated with nHz is most likely derived from Ca coordinated to carboxylate groups that may adhere to Hz during its release from the DV after schizogony. The carboxylate groups may derive from Hz surface or from proteins that may coordinate Ca in their structure, which are related to several vital functions for the development of the parasite and RBC invasion and egress [36]. Such proteins could be used as a target for the development of novel antimalarials [36].

As future work, the NEXAFS analysis could be extended to Si, Ca and P species on nHz using reference samples that best resemble their source and biological environment within the parasite. This analysis will help identify the inorganic species and their possible role in Hz biomineralization and in the immune modulation related to the crystals. A similar analysis could be also performed on Hz collected from other hematophagous parasites that produce Hz, such as *Schistosoma* or the bug of the triatomine species *Rhodnius prolixus*. This would determine if the inorganic species are preserved regardless of the parasite producing Hz, which in turn could provide further insights into their physiology and mechanism of survival.

4. Experimental

4.1. Materials

Reagent grade hexane, dichloromethane (DCM), sodium chloride, calcium chloride, ammonium chloride, sodium deoxycholate, and Igepal CA-630 were obtained from Sigma-Aldrich Canada. Sodium hydroxide pellets, hydrochloric acid ACS grade, and urea were purchased from Fisher Scientific. RPMI (Roswell Park Memorial Institute) medium 1640, gentamicin and L-glutamine were acquired from Gibco (Life Technologies), Halt protease inhibitor (single use cocktail, 100×), Proteinase K (20 mg/mL) PCR grade, and DNase I (100 U/mL) were purchased from ThermoFisher Scientific. Practical grade saponin from *Quillaja saponaria* Molina and *N*-2-hydroxyethylpiperazine-*N*′-2-ethanosulfonic acid (HEPES) were obtained from Acros Organics MS and sorbitol from Sigma life sciences. Phosphate buffer saline (PBS) tablets were purchased from BioShop, Canada Inc. A+ blood was purchased from The Interstate Blood Bank, INC.

Stock solutions of HEPES (25 mM), saponin (0.05%) in PBS (1×) and sorbitol (5%), PBS (1×, pH 7.4), Tris-HCl (10 mM, pH 8) were prepared in advance. 3-[(3-cholamidopropyl)dimethylammonio]-1-propanesulfonate hydrate (CHAPS) buffer (10 mM) was prepared by mixing NaCl (150 mM), $CaCl_2$ (1 mM) and the protease inhibitor in Tris HCl (50 mM), with the pH adjusted to 7.4. RIPA

(radioimmunoprecipitation assay) buffer was prepared using Tris HCl (50 mM, pH 7.4), Igepal CA-630 (1%), sodium deoxycholate (0.25%) and the protease inhibitor. Proteinase K (2 mg/mL) was prepared in a buffer solution of sodium dodecyl sulfate (SDS) (2%)/Tris-HCl, pH 8. DNase I (100 U/mL) was prepared in a buffer solution of Tris-HCl (10 mM), $MgCl_2$ (2.5 mM) and $CaCl_2$ (0.5 mM), pH 8.0. The pH of all the stock solutions was adjusted with HCl (0.1 M) or NaOH (0.1 M). Milli-Q water from a Barnstead purification system (resistivity of 18.2 MΩ-cm) was used to prepare all the solutions and experiments unless specified. Protein LoBind tubes were purchased from Eppendorf.

5. Methods

5.1. In vitro cultivation of P. falciparum and Hz extraction

Plasmodium falciparum of the CQ-sensitive strain 3D7-H and CQ-resistant strain 7G8 were cultivated in A+ human erythrocytes in hematocrit (2%) maintained in a synchronous culture with RPMI 1640 media supplemented with human plasma (10% v/v), L-Glutamine and HEPES (25 mM), as reported by Trager and Jensen's cultivation method [24b]. The parasitic blood stages were synchronized using sorbitol (5%), and the parasites were collected at the late trophozoite stage, followed by washes with PBS. Then, saponin (0.05%) in PBS was added to lyse the red blood cell, followed by washes with PBS and extraction with CHAPS (10 mM) or RIPA buffer. The lysates were centrifuged at 15 k rpm for 10 min, with the temperature controlled at 4 °C. The supernatant was removed, and the resulting Hz was resuspended in PBS and stored at 4 °C for further treatment.

5.2. Mice infection and Hz extraction

5.2.1. Parasites and animals

P. chabaudi AS was maintained in mice, by weekly passage, as described in the literature [16a]. Female C57BL/6 (B6) mice 8–12 weeks old, purchased from Charles River Laboratories, were infected intraperitoneally with parasitized RBCs (1×10^6). Infected B6 mice were sacrificed and spleens were harvested during peak parasitemia of > 35% parasitized RBC. Mice were maintained and handled according to the guidelines of the Canadian Council on Animal Care and the McGill University Animal Care Committee (ACC). All procedures performed on experimental mice were approved by the McGill University ACC (Protocol #2015–3750).

5.2.2. Preparation of splenic macrophages

Spleens from infected mice were perfused with complete RPMI 1640 medium (Life Technologies, Burlington, ON, Canada) supplemented with heat-inactivated fetal calf serum (FCS) (10%), HEPES (25 mM), gentamicin (0.12%), and glutamine (2 mM), and spleen tissues were pressed through a sterile steel mesh. Spleen cells were centrifuged, resuspended in ammonium chloride (0.175 M) to lyse red blood cells washed, counted and re-suspended in complete RPMI 1640 medium to 5×10^6 cells/mL and cultured in T-75 tissue culture flasks for macrophage adherence at 37 °C for 4 h with CO_2 (5%). Non-adherent cells were removed by washing the adherent cell layer with PBS. Adherent macrophages were lysed with 0.1% saponin, centrifuged, and the pellet collected.

5.2.3. Preparation of Hz from P. chabaudi AS infected splenic macrophages

Macrophage pellets obtained from steps described above washed in PBS and treated with SDS (2%) in endotoxin-free PBS followed by sonication for 20 s. After centrifugation, the pellet was resuspended in proteinase K (2 mg/mL) and incubated overnight at 37 °C. The digested product was washed 3 times with SDS (2%), resuspended in urea (6 M), and incubated on a shaker for 3 h at room temperature. After 3 washes in SDS (2%) and a PBS wash, the pellet was treated with DNase I (50 U/mL) for 1 h at 37 °C followed by heating to 95 °C for 10 min to inactivate DNase I. Finally, Hz crystals were washed twice with PBS and centrifuged at 15 k rpm for 10 min. Hz was resuspended in PBS and stored at 4 °C until further treatment.

5.3. Treatment of crude extracts of Hz with organic solvents

After collecting crude pellets of Hz obtained from both *P. falciparum* (Method 1) and *P. chabaudi AS* (Method 2), the crystals were subjected to alternative washes with hexane and DCM. Briefly, Hz pellet was centrifuged at 9 k rpm for 3 min and supernatants removed. Then, 1 mL of hexane was added to the mixture and sonicated for 30 s and centrifuged again at 9 k rpm for 3 min. This procedure was repeated using dichloromethane, followed by centrifugation at 9 k rpm for 5 min and the supernatant removed. Finally, Hz was treated again with hexane, centrifuged at 9 k rpm, the supernatant removed and dried at room temperature overnight and kept under vacuum until its analysis. The resulting material is referred as native Hz (nHz).

5.4. Characterization techniques

The atomic composition of nHz and the control samples were studied by X-ray photoelectron spectrometry (XPS) using a Thermo Scientific Kα spectrometer, equipped with a monochromated Al cathode with an incident Kα X-ray source (1486.6 eV, 0.843 nm), and an ultrahigh vacuum chamber (10^{-9} Torr). A flood gun of low energy electrons was used to prevent surface charging during the measurement. The analyses were carried out with a pass energy of 1 eV for all survey scans, and 0.1 eV for elemental high-resolution scans. Six points were randomly selected along each sample and at least three samples were analyzed. Quantitative analysis of the survey spectra and high-resolution spectra were fitted using Avantage Software version 5.956, using Gaussian-Voigt curve functions, and background removal through the Smart method. High-resolution spectral energies were normalized by fixing the position of the C-C/C=C component of C_{1s} at 284.5 eV.

The surface morphology and the elemental distribution of nHz samples were characterized by combining scanning electron microscopy (SEM) and energy-dispersive X-ray spectroscopy (EDS). The samples were mounted on an aluminum sample holder with carbon tape, followed by 8.5 nm of carbon coating (carbon sputter coater, EMS150R ES, Electron Microscopy Sciences (EMS)). The images were obtained using an Inspect-50 field emission scanning electron microscope (SEM) (FEI, Japan), operated in low vacuum mode, at 5 kV operating voltage. EDS spectra and elemental maps were acquired in the regions of interest using an EDX spectrometer (EDX, Thermo Scientific, USA).

5.5. Statistical analysis

Three independent experiments were performed for each Hz sample and at least two different spots were randomly selected and characterized along the same sample. All the data are expressed as mean ± standard deviation (SD). Means that are statistically different are indicated with a subscript asterisk (*). Microsoft Excel 2016 was used to perform statistical analysis. Unpaired *t*-test was performed to assess the statistic difference, where $P < 0.01$ was considered to be a significant difference.

Author contributions

E.D.G designed and performed the research, analyzed data and wrote the paper. F.B., O.G., and M.T. performed research. E.G. and M.M.S. wrote the paper. D.S.B. and M.C. designed the research, analyzed data and wrote the paper. All authors have given approval to the final version of the manuscript.

Notes

The authors declare no competing financial interest.

Acknowledgments

All the authors acknowledge the financial support from the Canada Research Chairs (CRC) foundation and Natural Sciences and Engineering Research Council of Canada (NSERC). EDG thanks Consejo Nacional de Ciencia y Tecnología (CONACyT) de México (CVU 354150), Secretaría de Educación Pública (SEP) de México (grant BC-3262) and the McGill Excellence Doctoral Award (MEDA) scholarships. FB also thanks to King Abdulaziz University - Saudi Arabia, in co-ordination with the Saudi Cultural Bureau – Ottawa for funding.

Appendix A. Supplementary data

Further details relative to materials and methods, XRD and FT-IR analysis of HA, and details relative to the parameters used for NEXAFS analysis of all samples. Supplementary data to this article can be found online at https://doi.org/10.1016/j.jinorgbio.2019.110808.

References

[1] T.J. Egan, Mol. Biochem. Parasitol. 157 (2008) 127–136.
[2] R. Stiebler, J.B.C. Soares, B.L. Timm, J.R. Silva, F.B. Mury, M. Dansa-Petretski, M.F. Oliveira, J. Bioenerg. Biomembr. 43 (2011) 93–99.
[3] S. Pagola, P.W. Stephens, D.S. Bohle, A.D. Kosar, S.K. Madsen, Nature 404 (2000) 307–310.
[4] K.A. de Villiers, M. Osipova, T.E. Mabotha, I. Solomonov, Y. Feldman, K. Kjaer, I. Weissbuch, T.J. Egan, L. Leiserowitz, Cryst. Growth Des. 9 (2009) 626–632.
[5] K.N. Olafson, T.Q. Nguyen, J.D. Rimer, P.G. Vekilov, Proc. Natl. Acad. Sci. 201700125 (2017).
[6] M. Boura, R. Frita, A. Góis, T. Carvalho, T. Hänscheid, Trends Parasitol. 29 (2013) 469–476.
[7] World Health Organization in *World malaria report, vol.* **2018**, (2018).
[8] L.M. Coronado, C.T. Nadovich, C. Spadafora, Biochimica et Biophysica Acta (BBA)-General Subjects 1840 (2014) 2032–2041.
[9] D.M. Newman, J. Heptinstall, R.J. Matelon, L. Savage, M.L. Wears, J. Beddow, M. Cox, H.D.F.H. Schallig, P.F. Mens, Biophys. J. 95 (2008) 994–1000.
[10] M. Giacometti, C. Rinaldi, M. Monticelli, L. Callegari, A. Collovini, D. Petti, G. Ferrari, R. Bertacco, Appl. Phys. Lett. 113 (2018) 203703.
[11] P. Parroche, F.N. Lauw, N. Goutagny, E. Latz, B.G. Monks, A. Visintin, K.A. Halmen, M. Lamphier, M. Olivier, D.C. Bartholomeu, R.T. Gazzinelli, D.T. Golenbock, Proc. Natl. Acad. Sci. 104 (2007) 1919–1924.
[12] M.T. Shio, F.A. Kassa, M.-J. Bellemare, M. Olivier, Microbes Infect. 12 (2010) 889–899.
[13] C.K. Carney, A.C. Schrimpe, K. Halfpenny, R.S. Harry, C.M. Miller, M. Broncel, S.L. Sewell, J.E. Schaff, R. Deol, M.D. Carter, JBIC Journal of Biological Inorganic Chemistry 11 (2006) 917–929.
[14] O.A. Skorokhod, M. Alessio, B. Mordmüller, P. Arese, E. Schwarzer, J. Immunol. 173 (2004) 4066–4074.
[15] C. Coban, K.J. Ishii, D.J. Sullivan, N. Kumar, Infect. Immun. 70 (2002) 3939–3943.
[16] a) N. Thawani, M. Tam, M.-J. Bellemare, D.S. Bohle, M. Olivier, J.B. de Souza, M.M. Stevenson, J. Infect. Dis. (2013) 140–149;
b) C. Casals-Pascual, O. Kai, J.O.P. Cheung, S. Williams, B. Lowe, M. Nyanoti, T.N. Williams, K. Maitland, M. Molyneux, C.R.J.C. Newton, N. Peshu, S.M. Watt, D.J. Roberts, Blood 108 (2006) 2569–2577;
c) O.A. Skorokhod, L. Caione, T. Marrocco, G. Migliardi, V. Barrera, P. Arese, W. Piacibello, E. Schwarzer, Blood 209 (1) (2010).
[17] P. Goldie, E.F. Roth, J. Oppenheim, J.P. Vanderberg, Am. J. Trop. Med. Hyg. 43 (1990) 584–596.
[18] E.D. Guerra, F. Baakdah, E. Georges, D.S. Bohle, M. Cerruti, J. Inorg. Biochem. 194 (2019) 214–222.
[19] J. Ashong, I. Blench, D. Warhurst, Trans. R. Soc. Trop. Med. Hyg. 83 (1989) 167–172.
[20] J.L. Green, R.R. Rees-Channer, S.A. Howell, S.R. Martin, E. Knuepfer, H.M. Taylor, M. Grainger, A.A. Holder, J. Biol. Chem. 283 (2008) 30980–30989.
[21] a) A. Klug, D. Rhodes, Trends Biochem. Sci. 12 (1987) 464–469;
b) W.B. Vernon, Magnesium 7 (1988) 234–248.
[22] J.I. Goldstein, D.E. Newbury, J.R. Michael, N.W. Ritchie, J.H.J. Scott, D.C. Joy, Scanning Electron Microscopy and X-Ray Microanalysis, Springer, 2017.
[23] J.B. Gilbert, M.F. Rubner, R.E. Cohen, Proc. Natl. Acad. Sci. 201222325 (2013).
[24] a) K. Tanabe, A. Izumo, K. Kageyama, The American Journal of Tropical Medicine and Hygiene 35 (1986) 476–478;
b) W. Trager, J.B. Jensen, J.P. Kreier (Ed.), Cultivation of Erythrocytic and Exoerythrocytic Stages of Plasmodia, Academic Press, 1980, pp. 271–319;
c) P.B. Dunham, G.W. Stewart, J.C. Ellory, Proceedings of the National Academy of Sciences 77 (1980) 1711–1715.
[25] P.M. Dietrich, C. Streeck, S. Glamsch, C. Ehlert, A. Lippitz, A. Nutsch, N. Kulak, B. Beckhoff, W. Unger, Anal. Chem. 87 (2015) 10117–10124.
[26] X. Guo, X. Liu, B. Xu, T. Dou, Colloids Surf. A Physicochem. Eng. Asp. 345 (2009) 141–146.
[27] a) E.M. Carlisle, Nutrition Reviews 40 (1982) 193–198;
b) J.D. Birchall, Chemical Society Reviews 24 (1995) 351–357.
[28] a) F. Balas, J. Pérez-Pariente, M. Vallet-Regí, Journal of Biomedical Materials Research Part A 66A (2003) 364–375;
b) Y. Tanizawa, T. Suzuki, Journal of the Chemical Society, Faraday Transactions 91 (1995) 3499–3503.
[29] H.-f. Li, S. Dimitrijev, D. Sweatman, H.B. Harrison, P. Tanner, B. Feil, J. Appl. Phys. 86 (1999) 4316–4321.
[30] a) D. Debona, F.A. Rodrigues, L.E. Datnoff, Annual Review of Phytopathology 55 (2017) 85–107;
b) Y. Alzahrani, A. Kuşvuran, H.F. Alharby, S. Kuşvuran, M.M. Rady, Ecotoxicology and environmental safety 154 (2018) 187–196;
c) J.F. Ma, N. Yamaji, Trends Plant Sci. 11 (2006) 392–397.
[31] V. Martin-Jézéquel, M. Hildebrand, M.A. Brzezinski, J. Phycol. 36 (2000) 821–840.
[32] F. Azam, S. Chisholm, Limnol. Oceanogr. 21 (1976) 427–435.
[33] K. Schwarz, Proc. Natl. Acad. Sci. U. S. A. 70 (1973) 1608–1612.
[34] C.H. Becker, A.G.S. Jánossy, Micron (1969) 10 (1979) 267–272.
[35] a) L.M. Jurkić, I. Cepanec, S.K. Pavelić, K. Pavelić, J. Nutr. metab. 10 (2013) 2 https://nutritionandmetabolism.biomedcentral.com/articles/10.1186/1743-7075-10-2;
b) J.M. Antonini, H.-M. Yang, J.Y. Ma, J.R. Roberts, M.W. Barger, L. Butterworth, T.G. Charron, V. Castranova, Inhal. Toxicol. 12 (2000) 1017–1036.
[36] S.N.J. Moreno, L. Ayong, D.A. Pace, Essays Biochem. 51 (2011) 97–110.
[37] G.A. Biagini, P.G. Bray, D.G. Spiller, M.R. White, S.A. Ward, J. Biol. Chem. 278 (2003) 27910–27915.
[38] B. Feng, J.Y. Chen, S.K. Qi, L. He, J.Z. Zhao, X.D. Zhang, Biomaterials 23 (2002) 173–179.
[39] J.F. Harper, A. Harmon, Nat. Rev. Mol. Cell Biol. 6 (2005) 555.
[40] R. Docampo, W. de Souza, K. Miranda, P. Rohloff, S.N.J. Moreno, Nat. Rev. Microbiol. 3 (2005) 251.
[41] R. Docampo, S.N.J. Moreno, Cell Calcium 50 (2011) 113–119.
[42] S. Hofmann in, Surface and Interface Analysis, John Wiley & Sons, Inc., 2000.
[43] O. Gourgas, J. Marulanda, P. Zhang, M. Murshed, M. Cerruti, Arterioscler. Thromb. Vasc. Biol. 38 (2) (2017) 363–372 (ATVBAHA. 117.309808).
[44] D. Eichert, M. Salomé, M. Banu, J. Susini, C. Rey, Spectrochim. Acta B At. Spectrosc. 60 (2005) 850–858.
[45] G. Pessi, G. Kociubinski, C.B. Mamoun, Proc. Natl. Acad. Sci. 101 (2004) 6206–6211.
[46] a) A. Samuels, A. Glass, D. Ehret and J. Menzies, *Annals of Botany* **1993**, *72*, 433–440.
b) S.B.A. Andrabi, M. Tahara, R. Matsubara, T. Toyama, H. Aonuma, H. Sakakibara, M. Suematsu, K. Tanabe, T. Nozaki, K. Nagamune, Parasitol. Int. 67 (2018) 47–58
[47] R. Jugdaohsingh, A.I.E. Watson, L.D. Pedro, J.J. Powell, Bone 75 (2015) 40–48.